Influence of the magnetization reversal mechanism on the electric field modulation of coercivity in Pt/Co structures

T. Koyama* and D. Chiba†

Department of Applied Physics, The University of Tokyo, Bunkyo, Tokyo 113-8656, Japan

(Received 14 November 2017; revised manuscript received 29 November 2017; published 7 December 2017)

We studied the effect of electric field (EF) on the coercivity of two Pt/Co structures with different Co layer thicknesses. Opposite signs of the coercivity change by the gate voltage application are observed in these samples, whereas the sign of the magnetic anisotropy change is the same. We performed direct observations of the domain structures during magnetization reversal under the gate voltage and found that two samples showed significant differences in the reversal process and EF effect. This result indicates that the sign reversal of the electric field effect on coercivity observed in the present structures originates from the difference in the macroscopic magnetization reversal process.

DOI: 10.1103/PhysRevB.96.224409

I. INTRODUCTION

Control of magnetic properties by electrical gating has been studied in ferromagnetic semiconductors [1–4] and, recently, in ferromagnetic metals [5–25]. The application of an electric field (EF) produces changes in the magnetic anisotropy (MA) [6,7,9,11–13], coercivity [5,10], Curie temperature [8], and exchange stiffness [14,15]. The microscopic origin of this effect is considered to be a modulation of the electronic structure at the Fermi level or the shift of that in the ferromagnetic materials by the gate voltage [16–19]. Previous research has reported that the sign of the EF effect depends on temperature [20], film-deposition condition [21], or film structure; e.g., an opposite sign of the MA modulation has been observed in the CoFeB/MgO structure with a different buffer layer [22]. This finding suggests that the microscopic electronic structure at the surface of the ferromagnetic layer plays an important role in determining the sign of the EF effect [23]. Our group also showed that the sign of the coercivity change in Pt/Co/MgO stacks depends on the sputter power for the MgO deposition [21].

Generally, the sign of the EF effect on the coercivity is the same as that on MA. In this study, however, we show that the sign of the coercivity change by EF is not always the same as that of MA. We proved this using two Pt/Co structures with different Co thickness t_{Co} deposited under the same conditions. The result of the direct observation of the magnetization reversal indicates that the dominant reversal process [domain nucleation or domain wall (DW) propagation] determines the sign of the coercivity modulation.

II. SAMPLE PREPARATION AND MEASUREMENT SETUP

Two Co/Pt structures with $t_{Co} = 0.69$ and $t_{Co} = 0.73$ (samples A and B, respectively) were deposited on thermally oxidized Si substrates using rf sputtering. The layer structure from the substrate side is as follows: Ta(2.7 nm)/Pt(2.0)/Co(t_{Co})/MgO(2.0). The layer thicknesses were determined from the deposition rates of each material. Xe gas was used during the deposition with a pressure of 0.2 Pa. The sputter power for the deposition of the MgO capping layer was 65 W [21]. The samples were fabricated into the Hall bar structure using photolithography and Ar ion milling. The widths of the wire for samples A and B were 20 and 30 μm, respectively. To apply a gate voltage V_G, a 50-nm-thick HfO_2 insulator layer and Cr(1.0)/Au(10) gate electrode were formed on each wire. The HfO_2 layer was deposited at 150°C using the atomic layer deposition technique.

Optical microscope images for samples A and B with measurement setups are shown in Figs. 1(a) and 1(b), respectively. Here, the positive sign of V_G corresponds to electron accumulation at the Co surface. The EF effect on the coercivity $\mu_0 H_c$ was investigated using the anomalous Hall effect in which the Hall resistance R_{Hall} is proportional to the perpendicular component of the magnetization. A dc current of 100 μA was applied to the wire to measure R_{Hall}. The measurements were performed at 300 K.

III. RESULTS AND DISCUSSION

Figures 2(a) and 2(b) show the results of the Hall measurement with a sweeping perpendicular field $\mu_0 H_\perp$ under V_G application for samples A and B, respectively. The vertical axes display R^n_{Hall}, the normalized R_{Hall}. The results for both samples show clear hysteresis loops, indicating that the samples have a perpendicular magnetic easy axis. In sample A, $\mu_0 H_c$ for $V_G = +15$ V is larger than that for -15 V. The direction of $\mu_0 H_c$ change produced by V_G in sample A is consistent with previously reported results for Pt/Co structures [8,21,24,25]. In contrast, $\mu_0 H_c$ decreases when the positive V_G is applied in sample B. These results clearly show that the signs of the EF effect on $\mu_0 H_c$ in samples A and B are opposite even though the t_{Co} difference is only 0.03 nm.

One factor for determining $\mu_0 H_c$ is MA, which is a more intrinsic magnetic parameter and expected to be linked directly to the electronic structure. Thus, the change in sign of $\mu_0 H_c$ between the two samples is likely attributable to the sign reversal of the MA modulation. Therefore, the EF effects on MA in the present samples were investigated as follows. The normalized in-plane magnetization (m^n_{inp}) curves

*tkoyama@ap.t.u-tokyo.ac.jp
†dchiba@ap.t.u-tokyo.ac.jp

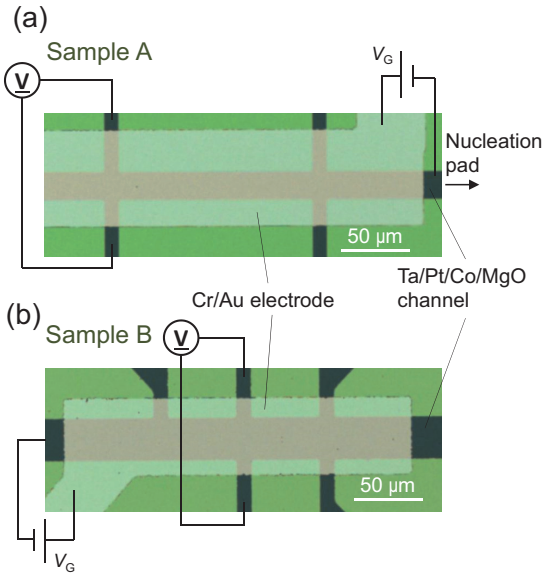

FIG. 1. Optical microscope images of the fabricated Hall bar structure of samples A (a) and B (b). A domain nucleation pad is attached to the right end of the wire in sample A.

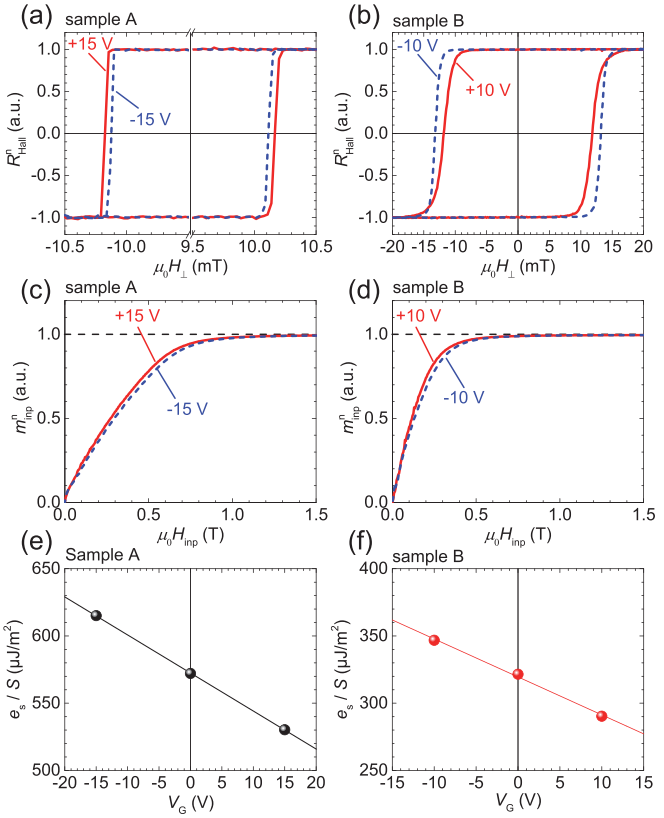

FIG. 2. (a,b) Results of the Hall measurements for samples A (a) and B (b). The vertical axes show the normalized Hall resistance R^n_{Hall}. (c,d) Normalized in-plane magnetization curves obtained with samples A (c) and B (d). (e,f) Perpendicular anisotropy energy per unit area e_k/S as a function of gate voltage V_G for samples A (e) and B (f). The solid line is the result of the linear fit.

for samples A and B are reproduced from the in-plane field $\mu_0 H_{inp}$ dependence of R_{Hall} as shown in Figs. 2(c) and 2(d) [25]. The in-plane saturation field ($\mu_0 H_k = 2\mu_0 \int H_{inp} dm^n_{inp}$) is calculated from the curves. Then, the perpendicular MA energy per unit area (e_a/S) is obtained from the following relation: $e_a/S = m_0 H_k m_s/2S$, where m_s/S is the saturation magnetic moment per unit area. m_s is measured using a superconducting quantum interference device magnetometer. Figures 2(e) and 2(f) show e_a/S as a function of V_G for samples A and B, respectively. The values of e_a/S for both samples, contrary to expectations, show negative correlations with V_G, indicating that the sign of the EF effect on the anisotropy is the same. Therefore, the opposite sign of $\mu_0 H_c$ modulation in the present samples cannot be explained simply from the MA modulation. From the slope of the linear fit, e_a/S modulation efficiencies are calculated to be 147 and 146 fJ/Vm for samples A and B, respectively. These results are quite consistent with one another. This finding suggests that the modulation of the electronic structure itself is expected to be similar in the two samples.

One important difference between samples A and B is the shape of the hysteresis curve; i.e., the magnetization switching is sharper in sample A than in sample B. The shape of the hysteresis curve for a system, as previously reported, reflects the magnetization process of the system; sharp switching is observed and the shape is nearly rectangular when the reversal is dominated by DW propagation, while a gradual switching can be seen in the case of the domain-nucleation-dominated reversal [26]. In order to check the detailed magnetization reversal process, the magnetic domain structure was observed using a magneto-optic Kerr effect (MOKE) microscope. The procedure of the observation includes several steps. First, by applying a large positive field, a single domain state with up magnetization was realized in both samples. Then, $\mu_0 H_\perp$ of −8.7 (−10.8) mT was constantly applied for sample A (B) and a series of MOKE images were obtained. In the case of sample A, a larger negative field is applied for 2 s immediately after the initialization, which creates the nucleated domain inside the nucleation pad attached to the right end of the wire, and then the field is set to be −8.7 mT. The contrast is enhanced by subtracting each image from the image taken at the initial state.

First, we show the sample A result, in which the same sign of $\mu_0 H_c$ change was observed. The successive MOKE images for $V_G = +15$ V during the application of $\mu_0 H_\perp = -8.7$ mT are shown in Figs. 3(a)–3(d). Figure 3(b) shows the result when a DW created in the nucleation pad flows into the wire from the right end of the wire; then Figs. 3(c) and 3(d) show a gradual movement of the DW to the left. This result clearly indicates that DW propagation dominates the magnetization reversal in sample A. A reversal via DW propagation is also confirmed when $V_G = -15$ V is applied. Figure 3(e) shows the DW velocity v for $V_G = \pm 15$ V measured under various values of perpendicular field $\mu_0 H_\perp$. The obtained v ranges from 10^{-4} to 10^{-5} m/s, corresponding to the thermally activated creep regime [27]. v for $V_G = -15$ V in the employed field range is always larger than that for $V_G = +15$ V, which is consistent with previous reports [24,25]. Therefore, when $V_G = +15$ V was applied, the time needed for the DW to arrive at the Hall cross increased. As a result, the value of $\mu_0 H_c$ appears to be larger for $V_G = +15$ V in sample A. We note that the amount of

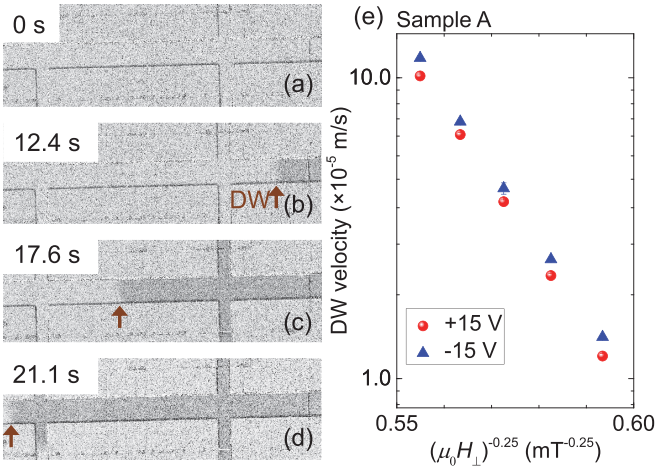

FIG. 3. (a) Magnetic domain images of sample A obtained using a magneto-optical Kerr effect (MOKE) microscope under an external perpendicular field $\mu_0 H_\perp$ of −8.7 mT. The position of the magnetic domain wall (DW) is indicated by the arrow. (b) Plot of the DW velocity v against $(\mu_0 H_\perp)^{-1/4}$ measured in sample A.

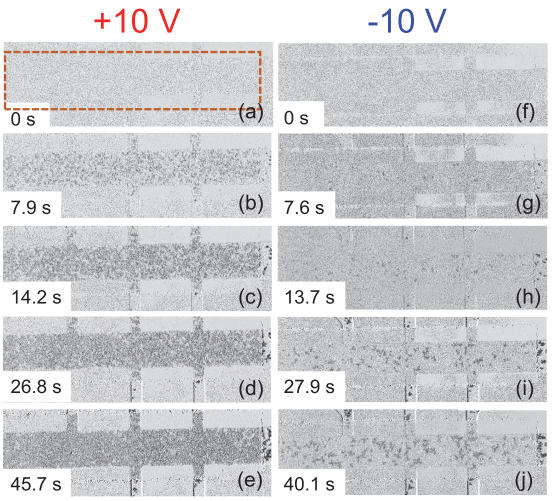

FIG. 4. MOKE images obtained in sample B under $\mu_0 H_\perp =$ –10.8 mT for $V_G =$ (a–e) + 10 V and (f–j) –10 V.

v change by EF in this study is smaller compared to previous reports [25]. This might be due to the difference in the Co layer thickness between sample A (0.69 nm) and the previous sample (∼0.4 nm).

Next, the MOKE images for sample B are shown in Fig. 4. Figures 4(a)–4(e) display the images taken under $V_G = +10$ V. Initially, the sample is a single domain state as Fig. 4(a) shows. After 7.9 s of application of $\mu_0 H_\perp = -10.8$ mT, a number of the small nucleated domains appear under the gate electrode [Fig. 4(b)]. Subsequently, as Figs. 4(c)–4(e) show, the magnetization reversal proceeds with the expansion of the nucleated domains and additional nucleation. This result suggests that in sample B the domain nucleation dominates the magnetization reversal. This finding agrees with the prediction from the shape of the hysteresis curve. Figures 4(f)–4(j) show the images taken under $V_G = -10$ V. One can see that at 7.6 s [Fig. 4(g)] the nucleation is rather sparse and the domain expands very slowly. This result suggests that the application of $V_G = -10$ V suppresses nucleation events and makes the magnetization reversal slower, resulting in the increase in $\mu_0 H_c$ by negative V_G in sample B. Domain nucleation is expected to occur in a thermally activated region [28,29]. In this case, the switching time τ for a single nucleation site follows the Arrhenius law [30]; $\tau = \tau_0 \exp(-E_a/k_B T)$, where τ_0 is the attempt frequency, E_a the activation energy, k_B the Boltzmann constant, and T the temperature. E_a depends on e_a/S and can be changed by V_G. When e_a/S increases (decreases) with negative (positive) V_G, τ becomes larger (smaller), resulting in the change in the nucleation rate. This can explain the EF effect on the reversal process observed in sample B. The magnetization reversal process in sample B observed here is strikingly different from the case of sample A (DW propagation). The smaller e_a/S in sample B (see Fig. 2) and some distribution of e_a/S in the plane of the sample may create the difference in the magnetization process. As a result, the different modulation mechanism (modulations of v or the domain nucleation rate) results in the opposite sign of the EF effect on $\mu_0 H_c$.

IV. CONCLUSION

In conclusion, we showed that the sign of the EF effect on the coercivity is not always the same as that of MA. The sign of the coercivity modulation can depend on the macroscopic reversal mechanism (DW propagation or domain nucleation). This finding suggests that only the coercivity modulation is inadequate for determining the sign of the EF effect on MA.

ACKNOWLEDGMENTS

The authors thank F. Matsukura and H. Ohno for their technical help. This work was partly supported by Grants-in-Aid for Young Scientists (A) (Grant No. 15H05419), Scientific Research (S) (Grant No. 25220604), Specially Promoted Research (Grant No. 15H05702) from JSPS (Japan), and Spintronics Research Network of Japan.

[1] H. Ohno, D. Chiba, F Matsukura, T. Omiya, E. Abe, T. Dietl, Y. Ohno, and K. Ohtani, Nature (London, UK) **408**, 944 (2000).
[2] D. Chiba, M. Yamanouchi, F. Matsukura, and H. Ohno, Science **301**, 943 (2003).
[3] D. Chiba, M. Sawicki, Y. Nishitani, Y. Nakatani, F Matsukura, and H. Ohno, Nature (London, UK) **455**, 515 (2008).
[4] N. Napel, M. O. Luen, J. M. Zavada, S. M. Bedair, P. Frajtag, and N. A. El-Masry, Appl. Phys. Lett. **94**, 132505 (2009).
[5] M. Weisheit, S. Fähler, A. Marty, Y. Souche, C. Poinsignon, and D. Givord, Science **315**, 349 (2007).
[6] T. Maruyama, Y. Shiota, T. Nozaki, K. Ohta, N. Toda, M. Mizuguchi, A. A. Tulapurkar, T. Shinjo, M. Shiraishi,

S. Mizukami, Y. Ando, and Y. Suzuki, Nat. Nanotechnol. **4**, 158 (2009).
[7] M. Endo, S. Kanai, S. Ikeda, F. Matsukura, and H. Ohno, Appl. Phys. Lett. **96**, 212503 (2010).
[8] D. Chiba, S. Fukami, K. Shimamura, N. Ishiwata, K. Kobayashi, and T. Ono, Nat. Mater. **10**, 853 (2011).
[9] Y. Shiota, T. Nozaki, F. Bonell, S. Murakami, T. Shinjo, and Y. Suzuki, Nat. Mater. **11**, 39 (2012).
[10] W.-G. Wang, M. Li, S. Hageman, and C. L. Chien, Nat. Mater. **11**, 64 (2012).
[11] S. Kanai, M. Yamanouchi, S. Ikeda, Y. Nakatani, F. Matsukura, and H. Ohno, Appl. Phys. Lett. **101**, 122403 (2012).
[12] J. Zhu, J. A. Katine, G. E. Rowlands, Y.-J. Chen, Z. Duan, J. G. Alzate, P. Upadhyaya, J. Langer, P. K. Amiri, K. L. Wang, and I. N. Krivorotov, Phys. Rev. Lett. **108**, 197203 (2012).
[13] U. Bauer, L. Yao, A. J. Tan, P. Agrawal, S. Emori, H. L. Tuller, S. Dijken, and G. S. D. Beach, Nat. Mater. **14**, 174 (2015).
[14] F. Ando, H. Kakizakai, T. Koyama, K. Yamada, M. Kawaguchi, S. Kim, K.-J. Kim, T. Moriyama, D. Chiba, and T. Ono, Appl. Phys. Lett. **109**, 022401 (2016).
[15] T. Dohi, S. Kanai, A. Okada, F. Matsukura, and H. Ohno, AIP Adv. **6**, 075017 (2016).
[16] C.-G. Duan, J. P. Velev, R. F. Sabirianov, Z. Zhu, J. Chu, S. S. Jaswal, and E. Y. Tsymbal, Phys. Rev. Lett. **101**, 137201 (2008).
[17] K. Nakamura, R. Shimabukuro, Y. Fujikawa, T. Akiyama, T. Ito, and A. J. Freeman, Phys. Rev. Lett. **102**, 187201 (2009).
[18] P. V. Ong, N. Kioussis, P. Amiri, J. G. Alzate, K. L. Wang, G. P. Carman, J. Hu, and R. Wu, Phys. Rev. B **89**, 094422 (2014).
[19] M. Oba, K. Nakamura, T. Akiyama, T. Ito, M. Weinert, and A. J. Freeman, Phys. Rev. Lett. **114**, 107202 (2015).
[20] Y. Hibino, T. Koyama, A. Obinata, T. Hirai, S. Ota, K. Miwa, S. Ono, F. Matsukura, H. Ohno, and D. Chiba, Appl. Phys. Lett. **109**, 082403 (2016).
[21] T. Koyama, A. Obinata, Y. Hibino, and D. Chiba, Appl. Phys. Exp. **6**, 123001 (2013).
[22] Y. Shiota, F. Bonell, S. Miwa, N. Mizuochi, T. Shinjo, and Y. Suzuki, Appl. Phys. Lett. **103**, 082410 (2013).
[23] R. Shimabukuro, K. Nakamura, T. Akiyama, and T. Ito, Phys. E (Amsterdam, Neth.) **42**, 1014 (2010).
[24] A. J. Schellekens, A. van den Brink, J. H. Franken, H. J. M. Swagten, and B. Koopmans, Nat. Commun. **3**, 847 (2012).
[25] D. Chiba, M. Kawaguchi, S. Fukami, N. Ishiwata, K. Shimamura, K. Kobayashi, and T. Ono, Nat. Commun. **3**, 888 (2012).
[26] U. Nowak, J. Heimel, T. Kleinefeld, and D. Weller, Phys. Rev. B **56**, 8143 (1997).
[27] P. J. Metaxas, J. P. Jamet, A. Mougin, M. Cormier, J. Ferré, V. Baltz, B. Rodmacq, B. Dieny, and R. L. Stamps, Phys. Rev. Lett. **99**, 217208 (2007).
[28] M. Labrune, S. Andrieu, F. Rio, and P. Bernstein, J. Magn. Magn. Mater. **80**, 211 (1989).
[29] A. Kirilyuk, J. Ferre, V. Grolier, J. P. Jamet, and D. Renard, J. Magn. Magn. Mater. **171**, 45 (1997).
[30] L. Néel, Sér. B **228**, 664 (1949).